Self-consistent Model Calculations of the Ordered S-matrix

and the Cylinder Correction

Jaime Millan[*,†,‡]

ABSTRACT

We study the multiperipheral ordered bootstrap of Rosenzweig
and Veneziano using dual triple Regge couplings exhibiting the required
threshold behavior. In the interval $-.5 \leqslant t \leqslant .8$ Gev^2 we obtain self-
consistent reggeon couplings and propagators for values of Regge slopes
and intercepts consistent with the physical values for the leading
natural-parity Regge trajectories. We calculate cylinder effects on
planar pole positions and couplings. By using an unsymmetrical planar
π-ρ reggeon loop model we are able to obtain self-consistent solutions
for the unnatural parity mesons in the interval $-.5 \leqslant t \leqslant .6$ Gev^2.
Neglecting effects of other Regge poles, our model gives a value of
the π-η splitting consistent with experiment.

TABLE OF CONTENTS

ACKNOWLEDGMENTS

I wish to express my sincere gratitude to Professor Geoffrey F. Chew for his invaluable advice, teaching and encouragement throughout my graduate studies.

Very illuminating discussions on the general subject of this research with Professors J. Kwiecinski and C. Rosenzweig and Mr. Philip Lutch are gratefully acknowledged. I am indebted to Drs. R. Donangelo and R. Ridell Jr. for help in matters of computer programming. At different stages of this work I benefited greatly from many conversations with fellow graduate students Dr. J.P. Sursock and Mr. G. Weissmann.

I should like to thank all the members of the theoretical group at the Lawrence Berkeley Laboratory for their friendship and hospitality. The help from Ms. Candy Voelker in getting this thesis ready for submission is deeply appreciated.

I want to express special appreciation to Drs. F. Arbab, E. Castellanos, C.J. Diaz, E. Guerrero, E. Gutiérrez, R. Kümmel, J. Marin, J. Roldan, A. Simar, M. Valero, R. Vargas and O. Zuñiga for very well-taught sequences of courses at Departamento de Física, Universidad del Valle, and most fruitful conversations and letters which greatly encouraged my interest in science. I should express heartful gratitude to my friends Amparo and Hernan Ortiz for their hospitality and encouragement during the period when this thesis was written.

I should like to express a sincere debt of gratitude to many other people, too numerous to mention by name, who with their teaching and friendship have helped me to take all the steps needed to reach this goal.

In particular, my wife Martha Ivett and my daughter Ximena have been a source of love, patience and encouragement throughout all these years. To them and to my mother Oliva is dedicated this thesis.

I. INTRODUCTION

In this work we want to report on results obtained in our efforts for constructing a self-consistent ordered S matrix and calculating cylinder renormalization effects. All of our considerations will be limited to the set of leading natural and unnatural-parity mesons only. To find consistent ordered Regge couplings and pole propagators we study numerically the multiperipheral bootstrap equation of Rosenzweig and Veneziano.[9] By properly incorporating the threshold behavior of the triple Regge couplings and by solving the ordered bootstrap at each value of t we are able to improve the results obtained by Schaap and Veneziano.[13] For the natural-parity trajectories we obtain self-consistent input-output solutions with values of intercepts and slopes consistent with their experimental values for t in the interval $-.5 \leqslant t \leqslant .8$ Gev[2]. We proceed then to calculate cylinder effects. We calculate cylinder shifts of Regge trajectories and their deviations from ideal behavior for the range of values of t for which ordered consistency was previously achieved. We apply similar methods to the leading unnatural-parity mesons by using an unsymmetrical reggeon-loop model for pseudoscalar reggeon couplings and propagators and we are able to obtain self-consistent solutions for $-.5 \leqslant t \leqslant .6$ Gev[2]. We then study the unnatural-parity cylinder, explain its overall sign and estimate its magnitude and behavior for small values of $|t|$. We calculate the $\pi-\eta$ splitting in the approximation in which lower-lying trajectories are neglected and obtain a result of the same order of magnitude as the experimental value.

This paper is organized as follows: in section II we summarize

the main physical ideas motivating the DTU approach. In section III
we describe the crucial properties of the ordered S matrix and in
section IV the planar S matrix is discussed. The Rosenzweig-Veneziano
ordered bootstrap is derived and studied in section V. Then, in
section VI, we calculate cylinder effects on vacuum planar Regge poles
and their couplings. Finally in section VII we present a model which
allows us to extend the DTU approach to the study of the unnatural-
parity mesons.

II. DUAL TOPOLOGICAL UNITARIZATION APPROACH
TO HADRON DYNAMICS

The Dual Topological Unitarization (DTU) scheme constitutes a
general framework developed for the purpose of constructing the
hadronic S-matrix. It was originally proposed by Veneziano and Chan
et al.[2] who, after realizing that dual resonance models (generalized
β-function and Neveu-Schwarz models) at the tree level exhibit several
regularities which are experimentally observed in the hadronic world
with fairly good accuracy, proposed a systematic unitarization proce-
dure to correct for the zero resonance width approximation inherent
to dual tree amplitudes. In their approach a dual tree connected part
is represented by a planar Harari-Rosner duality diagram as depicted
in Figure 1 and, assuming that amplitudes are determined from their
discontinuities, a planar dual theory is defined by summing first all
discontinuity contributions represented by planar-loop diagrams, as
illustrated in Figure 2. From this definition, a planar dual amplitude
exhibits the precious properties of the dual tree approximation.
Subsequent non-planar corrections are identified and classified
according to the topological structure of the corresponding quark-
duality diagrams[1,2]: after the planar amplitudes are constructed,
corrections having the topology of a cylinder are properly added next,
then diagrams having the topology of a torus and so on, as illustrated
in Figure 3. This systematic topological approach to unitarization
was first suggested by Veneziano,[1] who showed that with exact SU_N
internal symmetry successive components of the topological expansion
carry a convergence factor $(\frac{1}{N^2})^h$ (the effective value of N being about
2.5 at moderate energies), h representing the number of handles of the

minimal two-dimensional orientable surface in which the corresponding dual diagram can be embedded: $h=0$ for the leading planar term and the cylinder correction, $h=1$ for the torus, etc.

More recently, Chew and Rosenzweig and collaborators[3] have developed a more general approach going beyond dual resonance models. In brief, they propose to start from a sequentially-ordered Hilbert space H_0 in which the complete description of a channel requires besides the spin, momentum and type of each particle, the specification of the position that each one occupies in a sequence, the ordered asymptotic states in H_0 being connected by the ordered S matrix S_0, which turns out to be the generalization of the concept of a planar dual model. Then, a planar connected part is defined as the sum of the different ordered connected parts involving the set of particles participating in the hadronic process being described: this is the planar S matrix. The crucial property of the ordered S matrix is unitarity with respect to the ordered Hilbert space H_0. However, the planar S matrix, although representing a good approximation to the experimentally observed hadronic world, fails in exhibiting unitarity, and to recover this crucial property a topological expansion is formulated using particle diagrams along the same lines described previously.

DTU has produced remarkable results and opened up new ways of approaching old and new problems not only qualitatively but also at a more quantitative level: it has clarified the OZI-rule and its breaking patterns, the breaking of isospin and exchange degeneracy, the slope and intercept of the pomeron trajectory, the π-η mass split-ting, SU_3 symmetry breaking of Regge trajectories and couplings; it

has generated and clarified some of the results of quark models and, as suggested by Veneziano,[1] it may allow to find a relationship between QCD and S-matrix concepts. A complete description of DTU is given in reference 3 to which the interested reader is immediately referred.

III. THE ORDERED S MATRIX

1. Definition

In the approach of Chew and Rosenzweig to DTU[3] a sequentially-ordered Hilbert space H_0 is introduced at first. In this space the complete specification of an ordered channel requires that particles be given positions in a sequence. For example, the two-particle ordered asymptotic state $\left|\begin{matrix}A\\B\end{matrix}\right>$ is different from the state $\left|\begin{matrix}B\\A\end{matrix}\right>$, A and B denoting the quantum numbers of each particle. The ordered S-matrix S_0 connects two ordered asymptotic states and it can be represented as in Figure 4.

2. Properties

The ordered S matrix is supposed to possess the following properties:

a. *Unitarity with respect to H_0.* This property guarantees a consistent factorizable particle-pole spectrum from which DTU can begin safely: each of the two factors in the residue of a pole in an ordered connected part, denoted by R as , represented in Figure 5, is itself an ordered connected part, as shown in Figure 6.

b. *Ordered cluster decomposition.* This important property is illustrated in Figure 7 where the symbol R denotes an ordered connected part.

c. *Analyticity and ordered crossing.* Ordered connected parts are assumed to be analytic functions of the Mandelstam invariants on which they depend and, together with ordered unitarity, this guarantees the property of ordered crossing, illustrated in Figure 8 for a four-line ordered connected part: the single analytic function of diagram

(a) corresponds, for suitably chosen values of the invariants, to the four ordered transitions shown in diagrams (b), (c), (d), (e) but it does not correspond to transitions between the ordered channels (A,C) and (B,D) which are associated with different analytic functions.

d. *Absence of poles and normal thresholds in non-planar Mandelstam invariants.* An ordered connected part has no poles nor normal thresholds in channel invariants corresponding to sets of non-adjacent particles. Thus, the four-line ordered connected part shown in Figure 5 satisfies

$$\text{Disc}_{S_{AC}} R = \text{Disc}_{S_{BD}} R = 0 \tag{1}$$

and any general ordered connected part satisfies

$$\text{Disc}_{\text{Non-planar invariant}} R = 0.$$

IV. THE PLANAR S MATRIX

1. Definition

A planar connected part is defined as the sum of all possible ordered connected parts corresponding to the set of particles participating in the collision process, as shown in Figure 9 for a four-line connected part. This simple definition has the remarkable effect of eliminating the artificial notion of ordering in a given channel, allowing thus direct comparison of planar S matrix elements with experiment.

2. Properties of the planar S matrix

Because of its definition, the planar S matrix keeps many of the valuable properties of the ordered S matrix. For us, the most relevant properties are:

a. *Planar spectrum.* The planar S matrix inherits the factorizable pole-particle spectrum of the ordered S matrix which can be placed in direct correspondence with the physical particle spectrum because the restriction of order is irrelevant for a single-particle channel in H_0. From the topological constraints derived from ordered unitarity, Weissmann[4] has obtained the remarkable result that sequential ordering requires planar mesons to fall into families with $q\bar{q}$ quantum numbers, providing thus a justification for the use of quark diagrams. It is then possible to establish a correspondence between planar and physical mesons. From the SU_3 nonet groupings for the leading natural and unnatural parity mesons the following association follows:

Family	0^{-+}	1^{--}	2^{++}
d,u	π^+	ρ^+	A_2^+
s,u	K^0	K^0*	K^0**
s,d	$\bar{K}^+$	K^{+*}	K^{+**}
$\dfrac{1}{\sqrt{2}}(d,d+u,u)$	η	ω	f
$\dfrac{1}{\sqrt{2}}(d,d-u,u)$	π^0	ρ^0	$A_2^{\,0}$
ss	η^1	ϕ	f^1

   b. *Exchange degeneracy of planar Regge traj ·tories.* Consider
a four-line ordered connected part as in Figure 5. It does not have
poles and normal thresholds in the u-channel invariant. Ordered
amplitudes of opposite signature are than equal and, as a consequence,
ordered Regge trajectories of opposite signature coincide and have
equal ordered residues. However, in building the four-line planar
connected part six different ordered connected parts are superposed as
shown in Figure 9 and, therefore, a planar amplitude exhibits singulari-
ties in all channel invariants and planar amplitudes of opposite
signature are no longer equal. However, the positions of the ordered
Regge poles are not altered by the superposition and planar Regge
trajectories of opposite signature will continue being equal: this
is the property of exchange degeneracy of planar Regge trajectories.

   Experimentally, the leading natural-parity Regge trajectories
exhibit a remarkable pattern of exchange degeneracy. In the I=1 sector
the odd signature trajectory containing the $\rho(1^{--})$ and the $g(3^{--})$ and
the even signature trajectory going through the $A_2(2^{++})$ and the $h(4^{++})$
mesons are almost equal, the deviation being $\Delta J \approx 0.1$ at $t \approx 0$.   and

diminishing rapidly for growing values of t. A similar pattern is observed in the $I=\frac{1}{2}$ regge trajectories containing the $K^*(1^-)$ and the $K^{**}(2^+)$. The $I=0$ exchange degenerate partners, $\alpha_f - \alpha_\omega$ and $\alpha_\phi - \alpha_{f'}$, exhibit exchange degeneracy very accurately for $t \geqslant 0.5$ Gev² but the breaking is relatively large near $t = 0$.

For unnatural-parity trajectories there is less experimental evidence but it seems that the pattern of exchange degeneracy and its breakir , is the same as for the leading natural-parity meson trajec-tories

c. *Isospin degeneracy.* From isospin symmetry it follows that the combinations

$$\frac{1}{\sqrt{2}} \; [\; |d \, \bar{d} > \pm | \, u \, \bar{u} >]$$

corresponding to $I_z = 0$ for $I = 0$ and $I = 1$, must be degenerate. In the physical world the couples (ρ,ω) and (f,A_2) exhibit equality of masses and couplings with great accuracy. The pattern of breaking of isospin symmetry for Regge trajectories is very similar to that of exchange degeneracy, the breaking being large about $t = 0$ and diminish-ing rapidly as t grows positive.

d. *OZI selection rule.* Ordered selection rules such as charge conjugation invariance, together with topological restrictions imposed by ordered unitarity require non-vanishing ordered connected parts to be representable by single-boundary quark-line diagrams.[3,4] This constraint on ordered connected parts constitutes the explanation of the OZI selection rule[5,6,7] in the DTU approach: those reactions which cannot be depicted in terms of a connected quark-diagram are forbidden at the planar level of the topological expansion even if they are

allowed by internal quantum number conservation laws. Thus, as illus-
trated in Figure 10, at the planar level the process $\phi \to K^+ K^-$ is allowed
(Figure 10(a)) whereas the reaction $\phi \to \rho\pi$ is completely forbidden
(Figure 10(b)) but as shown in Figure 10(c) this last decay process
becomes allowed at the cylinder level. According to DTU the experi-
mentally small rates for OZI-rule forbidden processes are understood
as originated from non-planar corrections required to implement
unitarity of the full S matrix. A careful and complete review of the
experimental evidence supporting the OZI rule has been done by Okubo
in reference 8, where it is shown, for example, that processes such as
$\phi \to \rho\pi$ and $f^1 \to \pi\pi$ exhibit a dramatic suppression when compared to the
corresponding OZI rule-allowed process $\omega \to \rho\pi$ and $f \to \pi\pi$, respectively.
In this work, Okubo has also compiled evidence showing that reactions
involving η and η^1 exhibit a larger departure from the behavior required
by the OZI rule. According to DTU this is due to the fact, to be shown
later, that the cylinder correction is relatively large at the small
values of the masses of these pseudoscalar particles.

e. *Absence of Regge cuts and fixed-J poles in the planar S matrix.*
It has been conjectured, but not satisfactorily proven yet, that the
only singularities of the planar S matrix in the J-plane (Regge
singularities) are factorizable moving Regge poles. Branch points and
fixed poles are supposed to be absent at the planar level. The relative
weakness of Regge cuts finds the phenomenological support in the domi-
nance of short-range correlations in rapidity in multi-particle
production processes which can be understood as a consequence of
factorizable Regge poles, branch points being associated with long-
range rapidity correlations. This presumed simplicity of the Regge

singularity structure of ordered connected parts plays a very important role in the present attempts to calculate the ordered S matrix.

V. THE BOOTSTRAP OF THE ORDERED S MATRIX

1. Introduction

The cornerstone of the DTU approach to hadron dynamics is the ordered scattering matrix S_O. Starting from S_O, the planar S matrix is immediately obtained and this concept provides already a remarkably good approximation to the physical S-matrix. Also, the ordered S matrix fixes the higher order terms associated with non-planar effects in the topological expansion such as pomeron properties, breaking of exchange degeneracy and the OZI rule, etc. Therefore it is of crucial importance to the whole DTU approach to determine S_O. According to the bootstrap approach this is done by studying the infinite set of non-linear relations derived from ordered unitarity, the crucial property from which S_O should be uniquely determined.

2. The Rosenzweig-Veneziano ordered bootstrap

In this section we will describe the most promising model developed so far for the study of the bootstrap constraints derived from ordered unitarity, a model first proposed by Rosenzweig and Veneziano[9] and subsequently derived by several authors[10] using different approaches.

Consider an n-particle intermediate channel contribution to the s-discontinuity of a four-line ordered connected part R, as illustrated in Figure 11, where it is understood that the two ordered connected parts of the unitarity product are to be evaluated on opposite sides of the corresponding n-particle normal threshold. From previous experience with multiperipheral models it is known that in the region corresponding to large values of s and small values of t, the dominant contribution to the ordered connected part associated with the process

$\begin{pmatrix} A \\ B \end{pmatrix} \rightarrow \begin{pmatrix} 1 \\ 2 \\ : \\ N \end{pmatrix}$ comes from the so-called multiperipheral region of phase

space, characterized by small values of the momentum transfer invariants $t_1 \ldots t_{n-1}$, and which has the remarkable property that rapidity ordering $y_1 \geqslant y_2 \geqslant \ldots \geqslant y_n$ tends to coincide with particle ordering 1, 2, ... n. This is illustrated in Figure 12, in which we have assigned rapidities $-\frac{Y}{2}$ and $+\frac{Y}{2}$ to particles A and B respectively, and the intermediate n-particle state has been divided into two sets X_1 and X_2, the first set consisting of those particles having rapidities $y_i > 0$ and the set X_2 consisting of particles with rapidities $y_i < 0$. We make now the crucial assumption that the rapidity gap between the sets X_1 and X_2 is large enough to allow each ordered connected part appearing in the unitarity product to be expanded in terms of factorizable Regge poles, as illustrated in Figure 13, where the summation is to be performed over all possible ordered Regge poles. Later on in our analysis we will keep only the contributions from the leading poles in Regge expansions. In these conditions the summation over all values of n, the number of particles in the intermediate state, can be performed by summing independently over all possible values of n_1 and n_2, the number of ordered particles in each set X_1 and X_2 as shown in Figure 14(b). At this point we impose ordered unitarity for particle-reggeon ordered connected parts obtaining the result depicted in Figure 14(c).

In the asymptotic region $S \rightarrow \infty$ and t small a four-line ordered connected part is assumed to be dominated by a leading ordered reggeon $\alpha(t)$ and the s-discontinuity, corresponding to the left-hand side of Figure 11, is given then by the expression

$$A_4(s,t) = \pi \frac{\gamma_{AA^1}(t)\ \gamma_{BB^1}(t)}{\Gamma(\alpha(t))}\ S^{\alpha(t)} \tag{2}$$

the gamma function providing the sequence of nonsense zeros at
$\alpha(t) = 0, -1, -2, \ldots$, as for the leading physical ρ-trajectory. The
right-hand side of Figure 11 corresponds to the expression

$$\sum_{\alpha(t+),\alpha(t-)}\ \int d\phi_{\pm}\left[\left(\int_0^{s^1_{max}} ds^1\ A_{AA^1}(s^1,t,t_{\pm})\cdot D(\alpha(t_+))\ S^{\alpha(t+)}\ . \right.\right. \tag{(4)}$$

$$\left.\left. D^*(\alpha(t_-))S^{\alpha(t-)}\cdot\ \int_0^{s^1_{max}} ds^1\ A_{BB^1}(s^1,t,t_{\pm})\right] \tag{3}$$

where $\quad d\phi_{\pm} = \dfrac{1}{16\pi^4}\ \dfrac{dt_+\ dt_-\ \Theta(-\lambda(t,t_+,t_-))}{\sqrt{-\lambda(t,t_+,t_-)}}$

with $\lambda(t,\ t+,\ t-) = t^2 + t_+^2 + t_-^2 - 2t(t_+ + t_-) - 2t_+t_-$;

s^1 is the squared of the subenergy flowing through each reggeon–particle
discontinuity $A_{AA^1}(s^1,t,t\pm)$ and $A_{BB^1}(s^1,t,t\pm)$ each of which spans at
most half of the total rapidity interval and therefore $s^1_{max} \alpha\sqrt{S}$. The
symbols $D(\alpha(t+))$ and $D^*(\alpha(t-))$ represent the loop reggeon propagators
and they are given by the expressions

$$D(\alpha(t+)) = \Gamma(1-\alpha(t+))\ e^{i\pi\alpha(t+)}$$
$$D^*(\alpha(t-)) = \left[D(\alpha(t-))\right]^* \tag{5}$$

for $\alpha(t\pm)$ having its first physical particle-pole at $J = 1$, as the ρ
trajectory.

Assuming Regge behavior and the absence of branch points and fixed
poles in the J-plane in ordered connected parts, the following FESR is
· satisfied

$$\int_0^{s^1_{max}} ds^1 \; A_{AA^1}(s^1,t,t^\pm) \underset{s^1_{max} \to \infty}{\sim} \pi \; \frac{\gamma_{AA^1}(t)G(t,t^\pm)}{\Gamma(\alpha(t))} \; \frac{(s^1_{max})^{\alpha(t)-\alpha(t_+)-\alpha(t_-)}}{(\alpha(t)-\alpha(t_+)-\alpha(t_-)+1)} \quad (6)$$

where $G(t,t_+,t_-)$ is the s^1-discontinuity of the planar triple Regge coupling. When equation (6) is used in (3) together with the asymptotic relation $s^1_{max} \alpha \sqrt{S}$, the Rosenzweig-Veneziano multiperipheral ordered bootstrap condition is obtained:

$$\frac{1}{\Gamma(\alpha(t))} = \pi \sum_{\alpha(t_+),\alpha(t_-)} d\phi_\pm \frac{\left[G(t,t_+,t_-)/\Gamma(\alpha(t))\right]^2}{(\alpha(t)-\alpha(t_+)-\alpha(t-)+1)^2}$$

$$\Gamma(1-\alpha(t_+))\Gamma(1-\alpha(t_-)) \cdot \text{Cos}\pi(\alpha(t_+)-\alpha(t_-)) \quad (7)$$

an equation which is represented graphically in Figure 15.

3. Analytic solutions of the ordered bootstrap

The Rosenzweig-Veneziano bootstrap condition, equation (7), has the general form of a Dyson equation for the reggeon propagator:[11]

$$D_c(\alpha) = \pi \int d\phi_\pm \; \frac{1}{(\alpha-\alpha_c)^2} \; D_c(\alpha) \; G(\alpha,\alpha_+,\alpha_-) \cdot D(\alpha_+) \cdot D^*(\alpha_-) \cdot$$

$$\cdot \; G(\alpha,\alpha_+,\alpha_-) \cdot D_c(\alpha) \quad (8)$$

where $\alpha_c = \alpha(t_+) + \alpha(t_-) - 1$

$D(\alpha_+) = D(\alpha(t_+))$ is the reggeon bootstrap propagator,

$G(\alpha,\alpha_+,\alpha_-) = G(\alpha(t),\alpha(t_+),\alpha(t_-))$ is the triple Regge coupling introduced in equation (6) and $D_c(\alpha) = \frac{1}{\Gamma(\alpha(t))}$ is the s-discontinuity of the reggeon propagator (reggeon cut propagator). The bootstrap equation is a non-linear condition on the trajectory $\alpha(t)$ and the triple Regge coupling $G(\alpha(t),\alpha(t_+),\alpha(t_-))$.

Up to the present time it has not been possible to obtain analytic solutions of this equation in closed form. In reference 11 Bishari and Veneziano, based on the Dyson-form of equation (8), suggested the possibility of arriving at a solution through an iterative process in a way similar to reggeon calculus, which, as shown in reference 12, is intimately connected to DTU.

4. Numerical solutions of the ordered bootstrap

a. *The Schaap-Veneziano solution of the ordered bootstrap.* The study of quantitative solutions of the ordered bootstrap, in the form given in equation (7), was started by Schaap and Veneziano[13] with extremely encouraging results. They assumed triple Regge couplings to exhibit the form obtained in the generalized β-model,[14]

$$G(t,t_+,t_-) = \frac{g(t,t_+)\Gamma(\alpha(t))}{\Gamma(\alpha(t)-\alpha(t_+)-\alpha(t_-)+1)} \tag{9}$$

the function $g(t,t_+)$ being a constant in the tree approximation, and looked for self-consistent solutions for $\alpha(t)$ of linear form $\alpha(t) = \alpha(o) + \alpha^1 t$. They were justified in these steps because experimentally the leading Regge trajectories are linear in the small-t region and the dual tree model gives a non-trivial triple Regge vertex satisfying the analyticity and crossing requirements imposed by the concept of order. For example, the functional form (9) exhibits nonsense zeros at $\alpha(t) = \alpha(t_+)+\alpha(t_-)-1-N$ for $N = 0, +1, +2 \ldots$ which are required if Regge branch points are to be absent from ordered connected parts. In these conditions Schaap and Veneziano were able to show that if a linear input trajectory is inserted in the right-hand side of equation (7) and the left-hand side is represented as constant/$\Gamma(\alpha_{out})$, the input and output trajectories are approximately equal up to a best

choice of the constant, for values of the intercept satisfying
.57 $\leqslant \alpha(o) \leqslant$ .63 in the range $-.7 \leqslant \alpha^1 t \leqslant 0$. Their result is depicted
in Figure 16 for $\alpha(o) =$ .6.

b. *Solution of the ordered bootstrap with self-consistent Regge couplings.* The results of Schaap and Veneziano can be improved by
incorporating the threshold behavior of Regge residues, as first
suggested by Chew and Rosenzweig.[15] The threshold barrier effect can
be seen already in the Froissart-Gribov projection for a t-channel
partial-wave amplitude:[16]

$$A_J(t) = \int_{Z_t(t,s_0)}^{\infty} Q_J(Z_t^1) D_s(t,s^1) dZ_t^1$$

where $Z_t^1 = 1 + \frac{s^1}{2q_t^2} \rightarrow \frac{s^1}{2q_t^2}$ when $q_t^2 \rightarrow 0$. For large values of
Z_t^1 the rotation group projection function $Q_J(Z_t^1)$ has the behavior
$Q_J(Z_t^1) \underset{Z_t^1 \rightarrow \infty}{\sim} (Z_t^1)^{-(J+1)}$ and therefore $A_J(t) \alpha (q_t^2)^J$ as $q_t^2 \rightarrow 0$, provided the
discontinuity function $D_s(t,s^1)$ behaves smoothly.

The generalization to a multiperipheral helicity-pole loop involv-
ing triple Regge couplings has been studied in Reference 16. It is
shown there that the set of variables most suitable for an exact
treatment of the problem is the couple (k,ω), related to the variables
(t_+, t_-) by the equations

$$k^2 = \frac{\lambda(t, t_+, t_-)}{4t}$$

$$\omega = \frac{(t_+ - t_-)}{2\sqrt{-t}} \tag{10}$$

$$t_\pm = \frac{t}{4} - k^2 - \omega^2 \pm \omega\sqrt{-t}$$

where $\lambda(t,t_+,t_-)$ is the triangular function defined previously and k^2 represents the squared magnitude of the t-channel overall momentum flowing around the loop. In terms of these variables, the threshold behavior of the triple Regge vertex is

$$G(t,t_+,t_-)=G(\alpha(t),\alpha(t_+),\alpha(t_-))=G(J_1 t,k^2,\omega^2)+\left(\frac{k^2}{M^2}\right)^{J-\alpha(t_+)-\alpha(t_-)+1} \tag{11}$$
$$J=\alpha(t)$$
$$k^2 \to 0$$

From the point of view of the s-channel, the threshold behavior represents the lower limit constraint on $t^{\pm}$ (t_{min}-effects).

As properly pointed out in reference 17, in weak-coupling models based on a Mellin-transform approach to the J-diagonalization of the multiperipheral integral equation, the output Regge pole occurs very close to the branch point, according to the relation

$$<J-\alpha(t_+)-\alpha(t_-)+1> \approx g^2$$

and therefore threshold barrier-effects can be easily overlooked.

In looking for self-consistent solutions to the ordered bootstrap equation (7), we have used the following functional form to incorporate the required threshold behavior of the couplings:

$$T(J,t,U;M^2) = \left(\frac{U}{M^2}\right)^{J+1} \left(tgh\,\frac{U}{M^2}\right)^{-1-\alpha_c(t_+,t_-)} \tag{12}$$

where $U = k^2+\omega^2$ and $\alpha_c(t_+,t_-) = \alpha(t_+)+\alpha(t_-)-1$. This interpolating function allows us to keep the peripheral properties of the dual tree approximation which are important to guarantee a strong damping of the integrand as k and $|\omega|$ take large values. At the same time, we are able to avoid unwanted singularities which appear when the form $\left(\frac{k^2}{M^2}\right)^{J-\alpha_c}$ is used, as can be easily verified at $t = 0$. This function $T(J,t,u;M^2)$ is introduced as a multiplicative factor in the expression

for the triple Regge coupling and can be associated with the function $g(t,t_+,t_-)$ appearing in Eq. (9). An additional smooth t-dependence of the Regge coupling will be required when solving the ordered bootstrap at each value of t, as will be shown later.

We proceed to study the ordered bootstrap in the same way as Schaap and Veneziano did it in reference 13. The trajectory functions are assumed to be linear $\alpha(t)=\alpha(0)+\alpha^1 t$, the values of the slopes and intercepts being left as free parameters (together with the scale factor M^2 appearing in the triple Regge vertex) to be fixed by overall self-consistency. In these conditions it becomes possible to obtain solutions for the ordered trajectories $\alpha_{\rho-f}$, α_{k*} and $\alpha_{\phi-f^1}$ exhibiting SU_3 symmetry breaking in the values of their intercepts and slopes.

In the approximation in which only the highest-lying Regge poles are kept in the reggeon loops, the ordered bootstrap condition becomes a set of coupled-channel equations.[17] Using the notation

$$\begin{bmatrix} a \\ b \quad c \end{bmatrix} = \int d\phi_\pm \frac{\left[G(t,t_+,t_-)/\Gamma(\alpha_a(t))\right]^2}{(\alpha_a(t)-\alpha_b(t_+)-\alpha_c(t_-)+1)^2} \Gamma(1-\alpha_b(t_+))\Gamma(1-\alpha_c(t_-)) \cdot$$

$$\cdot \cos\pi(\alpha_b(t_+)-\alpha_c(t_-)) \tag{13}$$

the coupled-channel equations are

$$\frac{1}{\Gamma(\alpha_\rho(t))} = 2 \begin{bmatrix} \rho \\ \rho \quad \rho \end{bmatrix} + \begin{bmatrix} \rho \\ K* \quad K* \end{bmatrix}$$

$$\frac{1}{\Gamma(\alpha_{K*}(t))} = 2 \begin{bmatrix} K* \\ K* \quad \rho \end{bmatrix} + \begin{bmatrix} K* \\ K* \quad \phi \end{bmatrix} \tag{14}$$

$$\frac{1}{\Gamma(\alpha_\phi(t))} = 2 \begin{bmatrix} \phi \\ K* \quad K* \end{bmatrix} + \begin{bmatrix} \phi \\ \phi \quad \phi \end{bmatrix}$$

A very restrictive condition to be satisfied originates from the nonsense zeros present in the left-hand side of equations (14) at values of t satisfying $t_0 = -\alpha_a(o)/\alpha_a^1$, which depend on both the intercept and the slope of the input trajectories. Each of these zeros is to be balanced by a corresponding zero in the right-hand side generated from a sign change of the average value of the oscillating factor $\xi = \text{Cos } \pi(\alpha_b(t_+)-\alpha_c(t_-))$ present in each loop integrand. For each separate loop in the right-hand side of Eqs. (14) the value of the parameter M^2 is fixed by requiring its sign change to occur at the value $t = t_0$ already fixed by the slope and intercept of $\alpha_a(t)$. Furthermore, when considering the equation for the $f^1-\phi$ planar trajec- tory for intercept values of the order of .25 it is necessary to introduce slope values smaller than 1. Gev^{-2}, because the relevant loops in the right-hand side tend to change sign at negative t-values satisfying $|t| > \alpha_\phi(o)$.

The exact t-dependence of the triple Regge vertex function is obtained by solving the bootstrap equation at each value of t. Consider for example the bootstrap condition for the leading planar ρ-f trajectory when written in the form

$$1 = \Gamma(\alpha_\rho(t)) \left\{ 2 \begin{bmatrix} & \rho & \\ \rho & & \rho \end{bmatrix} + \begin{bmatrix} & \rho & \\ K* & & K* \end{bmatrix} \right\} \equiv P(t) \qquad (15)$$

Let us assume the following form for the triple Regge vertex squared:

$$G^2(J,t,t_+,t_-) = T(J,t,u,M^2) \left[\frac{g(t)\Gamma(\alpha(t))}{\Gamma(\alpha(t)-\alpha_c(t_+,t_-))} \right]^2 \qquad (16)$$

Choosing $g(t) = g(o) = \text{constant}$, by requiring Eq. (15) to hold at $t = 0$ and calculating the function $P(t)$, the right-hand side of Eq. (15), for several values of t we obtain the values corresponding to the dashed

line in Figure 17. It is then obvious that the degree of accuracy within which Eq. (15) is satisfied can be improved by considering the functional form $g(t) = g(o) e^{-at}$ and choosing properly the value of the parameter a. It becomes possible to satisfy the bootstrap condition not only for negative -t but also over a substantial interval of positive t-values. In these conditions we have been able to solve the set of coupled equations (14) achieving self-consistency within 10% for input intercepts in the range $.25 \lesssim \alpha(o) \lesssim .65$ and slopes in the interval $.6 < \alpha^1 < 1.$ with $M^2 \approx 0.5 - 0.8$ and $a \approx .50 - .65$ for values of t in the interval $-.5 \leqslant t \leqslant .8$ Gev^2.

Eventually ordered unitarity will allow a complete determination of all the free parameters such as a and M^2. Konishi and Kwiecinski[18,19] have already made great progress by deriving bootstrap equations for triple and double Regge vertices, which when combined with the Rosenzweig-Veneziano self-consistency condition for the propagator, should allow only a discrete set of solutions for trajectory slopes and intercepts, determining in this way the set of planar Regge trajectories and couplings.

VI. THE CYLINDER CORRECTION TO THE PLANAR S MATRIX

1. Renormalization of vacuum planar Regge poles by the cylinder

According to DTU the leading correction to the (non-unitary) planar
S matrix corresponds to non-planar discontinuity products which can be
embedded in a two-dimensional surface having the topology of a cylinder
as illustrated in Figure 3(a). The properties of the cylinder correc-
tion have been extensively studied by several authors.[3] It has been
shown that the cylinder renormalizes the position and residues of planar
Regge poles carrying zero additive quantum numbers, while those
trajectories such as the $\rho-A_2$ (I=1), the K^*-K^{**} (I=½) or the $\pi-B$ (I=1)
which carry non-zero additive quantum numbers are not shifted at all
from their planar values. The positions and residues of poles of
opposite charge conjugation are renormalized in opposite directions.
The even charge-conjugation planar f-trajectory, carrying quantum
numbers corresponding to $u\bar{u}$ and $d\bar{d}$ quark combinations, is shifted
upwards, near t=0, by the cylinder; it gains some $s\bar{s}$ mixture and
becomes closer to an SU_3 singlet. The cylinder-shifted f is the pomeron
according to Chew and Rosenzweig.[19] The I=0 negative charge-conjugation
ω-trajectory, exchange-degenerate partner of the f, is renormalized in
the opposite direction by the cylinder. Similarly, the even charge
conjugation f , purely $s\bar{s}$ at the planar level is shifted upwards
adquiring $u\bar{u}$ and $d\bar{d}$ components, its odd charge conjugation planar
partner, the ϕ trajectory, being renormalized downwards.

2. A model for cylinder poles

The description of the properties of cylinder-shifted Regge poles
for the set of leading natural-parity trajectories is most easily

approached in terms of a simple model proposed by Chew and Rosenzweig in reference 18. In this model the cylinder correction to the planar S matrix is described by a twist operator C(t) with matrix elements in the space of planar Regge poles depicted as in Figure 18(a), the index i denoting the sequence of planar Regge poles. In this model two simplifying assumptions are made: (i) the influence of lower-lying trajectories on the set of leading planar mesons is neglected. This may not be a good approximation especially for the ϕ trajectory which can be affected by lower-lying trajectories such as baryon or baryonium states, as conjectured by several authors.[3,21] (ii) All SU_3 symmetry-breaking is placed in pole positions by taking different intercepts for the planar trajectories α_ρ, α_{K*} and α_ϕ but the cylinder couplings are assumed to be SU_3 symmetric.

In the I=0 sector of leading planar poles, the planar propagator and the cylinder twist operator are described by matrices $\underline{P}$ and C with

$$P = \begin{pmatrix} \dfrac{1}{J-\alpha_0} & 0 \\ 0 & \dfrac{1}{J-\alpha_3} \end{pmatrix} \qquad C = \pm k \begin{pmatrix} 2 & \sqrt{2} \\ \sqrt{2} & 1 \end{pmatrix}$$

$\alpha_0 = \alpha_0(t)$ and $\alpha_3 = \alpha_3(t)$ being the ρ-f and the ϕ-f^1 planar trajectories, the parameter k depending on t and J- the position of the output cylinder pole. In reference 19 it is shown that even charge-conjugation cylinder poles are shifted from their planar positions according to the expression

$$\alpha_{f,f^1} = \tfrac{1}{2} \left\{ \alpha_0 + \alpha_3 + 3k \pm \left[(\alpha_0 - \alpha_3 + k)^2 + 8k^2 \right]^{\tfrac{1}{2}} \right\} \qquad (17)$$

while the new odd change-conjugation trajectories ω and ϕ are given by a similar formula with k replaced by (-k) in Eq. (17). Designating by

$|0\rangle$ and $|3\rangle$ the original I=0 planar basis states, corresponding to the trajectories α_0 and α_3 respectively, the new states of even charge conjugation are

$$|f\rangle = \cos \theta^+ |0\rangle + \sin \theta^+ |3\rangle$$
$$|f^1\rangle = -\sin \theta^+ |0\rangle + \cos \theta^+ |3\rangle$$

where $\tan 2\theta^+ = \dfrac{\sqrt{8}k}{(\alpha_0 - \alpha_3 + k)}$ \hfill (18)

The odd charge-conjugation states $|\omega\rangle$ and $|\phi\rangle$ are given by corresponding formulas with a mixing angle θ^- determined from these equations with k replaced by $(-k)$.

3. Helicity-pole model for the twisted cylinder loop

According to the considerations of the preceeding section, cylinder effects on planar Regge poles and residues can be economically described in terms of a unique parameter $k(J,t)$ which is determined from the ordered S matrix through self-consistent planar triple Regge couplings. Lutch[16] has given complete meaning to the twisted dual diagram of Figure 18(a), associated with the cylinder, through a helicity-pole expansion corresponding to the reggeon loop depicted in Figure 18(b).

From the fact that unitarity demands complete cylinder amplitudes (the sum of planar and cylinder amplitudes) to exhibit factorizable Regge poles with neither Regge cuts nor fixed-J singularities, Tuan and Freeman,[20] independently, have proposed the following expression for the twisted reggeon loop parameter $Nk(J,t)$:

$$Nk(J,t) = \pi N \int d\phi_{\pm} \quad \frac{G^2(J,t,t_+,t_-)}{\alpha(t) - \alpha_c(t_+,t_-)} \Gamma(1-\alpha(t_+))\Gamma(1-\alpha(t_-)) \qquad (19)$$

the absence of a factor $(J-\alpha_c)^{-1}$ been required to avoid Regge cuts at the cylinder level.

4. Quantitative calculation of cylinder effects

Because we have obtained a fully self-consistent ordered bootstrap model for the set of leading planar Regge poles we can proceed to calculate cylinder effects. However an exact calculation would require the incorporation of SU_3 symmetry-breaking effects on twisted-reggeon loops and the solution of coupled non-linear equations to find the positions of cylinder poles. We will follow a simpler but approximate method by solving first the non-linear equation (17) for the f-trajectory in the approximation in which only planar ρ-helicity poles are kept in the twisted reggeon links of Figure 18(b), this approximation being consistent with the assumption of SU_3 symmetric cylinder couplings. In this way we find the value of the parameter $k(t)$ at different values of t, and these values are used then to calculate the cylinder shifted trajectories and mixing angles by using equations (17) and (18). The results obtained are exhibited in Figures 20 and 21 for a set of typical planar trajectories

$$\alpha_0 = \alpha_\rho(t) = .5 + .95t$$
$$\alpha_2 = \alpha_{K*}(t) = .4 + .91t$$
$$\alpha_3 = \alpha_\phi(t) = .3 + .71t$$

for which full consistency was achieved at the ordered level. The continuous line in Figure 19 displays the values of the parameter $3k(t)$ in the range of values of t within which we obtained self-consistent planar couplings. Near t=0, $3k \approx .30$ and it decreases rapidly in the positive-t region while it increases very fast in the small negative-t direction.

The resulting spectrum of cylinder Regge trajectories is shown by the continuous lines of Figure 20, the dashed lines representing the

input planar Regge poles already described. The f-trajectory is shifted upwards, its intercept becomes $\alpha_f(o) = .81$ and its slope is now $\alpha_f^1(o) \approx .4$, becoming even flatter in the negative-t side. As t grows positive, it approaches rapidly the planar ρ-trajectory. The ω-trajectory is renormalized downwards from its planar values, its intercept becomes $\alpha_\omega(o) = .40$. Similarly, the f^1 is slightly shifted in the upward direction and $\alpha_{f1}(o) = .34$ while the ϕ is shifted downwards to $\alpha_\phi(o) = .1$.

At this point we want to remark on the importance of the J-dependence of the twisted reggeon-loop associated with the cylinder, coming from threshold barrier effects of the form $\left(\dfrac{k^2}{M^2}\right)^{J-\alpha_c}$ as discussed previously. If this J-dependence is ignored the value of the intercept of the f-trajectory turns out to be uncomfortably high, of the order of 1.5 units.

From the values of $k(t)$ we can also calculate $\tan\theta\pm$ at each value of t, according to formula (18). The results are shown in Figure 21, which shows that cylinder mixing decrease for positive values of t and the cylinder-normalized states approach their ideal nonet planar structure.

Our results show good agreement with those obtained by Tsou in reference 21 using an iterative approach to the calculation of cylinder effects and a different parametrization for triple Regge couplings, with parameters extracted directly from phenomenological input. The results obtained by Tsou are in satisfactory agreement with experimental data and this allows us to be optimistic as to the possibility of obtaining phenomenologically realistic Regge couplings and trajectories directly from ordered bootstrap constraints.

VII. EXTENDING DTU TO THE UNNATURAL-PARITY MESONS

1. Introduction

It is an empirical fact that the physical pseudoscalar mesons π, η and η^1 display a departure from the planar behavior which is strikingly different from the deviation exhibited by the vector and tensor mesons ρ, ω, ϕ and A_2, f, f^1. For example, comparing particles of even charge conjugation, the I=0 f is less massive than the I=1 A_2 by about 40 Mev but the I=0 η is more massive than the I=1 π by about 400 Mev; similarly the deviation from isospin degeneracy and the breaking of exchange degeneracy are much larger for the unnatural-parity than for the natural-parity trajectories. The mixing patterns between these two sets of mesons also reveals large differences between them: the nonet mass-formula $m(\omega) = m(\rho)$ and $m^2(K^*)-m^2(\rho) = m^2(\phi)-m^2(K^*)$ is experimentally fairly well satisfied but the pseudoscalar nonet formula $m(\eta) = m(\pi)$ is very badly violated.

As shown in references 22, DTU offers the possibility of explaining at a qualitative and quantitative level the properties of the pseudoscalar mesons. The π-η mass splitting, the η-η^1 mixing pattern and the large violations of the OZI rule observed in their decays, are just different manifestations of the same fact: unnatural-parity cylinder effects are large in the low-mass region. In the next sections we will study a simple model that illustrates the rich potentialities offered by DTU for the study and understanding of the properties of the pseudoscalar mesons.

2. Unnatural-parity planar spectrum

The general considerations regarding the ordered S matrix and the

cylinder correction previously applied to the leading vector and tensor trajectories can be immediately extended to the unnatural-parity mesons.[22] The starting point is the assumption that the planar spectrum exhibiting exchange and isospin degeneracy consists of three equally-spaced Regge trajectories α_0, α_2 and α_3, the leading trajectory α_0 corresponding to $u\bar{u}$ and $d\bar{d}$ quantum numbers and containing the I=0 η and H and the I=1 π and B mesons, the trajectory α_1 containing the strange I=$\frac{1}{2}$ K and Q mesons, while the trajectory α_3 corresponds to $s\bar{s}$ and contains the I=0 η^1 and H^1 mesons.

3. Multiperipheral ordered bootstrap model for unnatural-parity mesons

The problem of achieving a consistent ordered bootstrap for the pseudoscalar mesons is even more difficult than for the natural-parity mesons. The most promising approach follows the lines first suggested by Chew and Rosenzweig,[15] who proposed that the reggeon-loop model relevant in a neighborhood about t=0 corresponds to the unsymmetrical loop depicted in Figure 22, parity conservation requiring one link to carry natural-parity and the other link unnatural-parity.[23] We will consider only the approximation in which lower-lying trajectories that carry strangeness, such as K^*, η^1, are neglected.

According to this model the Rosenzweig-Veneziano bootstrap condition takes the form

$$1 = \pi N \int d\phi_{\pm} \quad \frac{\left[G(t,t_+,t_-)/\Gamma(1+\alpha_\pi(t))\right]^2}{\left[\alpha_\pi(t)-\alpha_c(t_+,t_-)\right]^2} \quad \Gamma(-\alpha_\pi(t_+))\Gamma(1-\alpha_\rho(t_-)) \cdot$$

$$\cdot \cos \, \pi(\alpha_\pi(t_+)-\alpha_\rho(t_-)) \qquad (20)$$

where $\alpha_c(t_+,t_-) = \alpha_\pi(t_+) + \alpha_\rho(t_-)-1$ \qquad (21)

and $G(t,t_+,t_-) = \dfrac{g(t,t_+,t_-)\Gamma(1+\alpha_\pi(t))}{\Gamma(\alpha_\pi(t)-\alpha_\pi(t_+)-\alpha_\rho(t_-)+1)}$ (22)

is the triple Regge vertex.

Let us describe now some considerations which are relevant when attempting to find a self-consistent planar triple Regge vertex for the unsymmetrical reggeon-loop model under study. From Eq. (2) we immediately notice that if the quantity $\delta = (\alpha_\rho(o)-\alpha_\pi(o))-0.5$ vanishes exactly then the loop integral will be zero at t=0, because of the planar reggeon phase factors. In general the parameter δ will be determined from the ordered self-consistency conditions but we will consider it as a free parameter adopting small positive values, the loop integral vanishing then at a small negative value of t. Chew has proposed to interpret this zero as being the analog of the nonsense zero occurring at $t \approx -0.5$ in the symmetrical loop relevant to the bootstrap of the leading natural-parity ρ-f trajectory which also had its origin in the planar reggeon phase factors, overall self-consistency at this particular value of t being achieved by the presence of a matching zero in the cut planar reggeon propagator $D_c(\alpha) = 1/\Gamma(\alpha)$ and a simultaneous pole and nonsense zero present in the planar triple Regge vertex. That overall self-consistency imposes these powerful analyticity constraints on planar reggeon couplings and propagator is very nicely exhibited by the ordered bootstrap equation when written in the form (8).

Extension of these prescriptions to the unnatural-parity case leads us to propose the following forms for the reggeon propagator and the triple Regge vertex:

$$D_c(\alpha) = 1 \ / \ \Gamma(1+\alpha_\pi(t))\Gamma(\alpha_\pi(t)-\epsilon) \qquad (23)$$

$$G(t,t_+,t_-) = \frac{\Gamma(1+\alpha_\pi(t)) \cdot g(t,t_+,t_-)}{\Gamma(\alpha_\pi(t)-\alpha_\pi(t_+)-\alpha_\rho(t_-)+1)} \cdot \frac{\Gamma(\alpha_\pi(t)-\epsilon)}{\Gamma(\alpha_\pi(t)-\epsilon-\alpha_\pi(t_+)-\alpha_\rho(t_-)+1)} \qquad (24)$$

Eq. 23 exhibits a zero in the pion propagator at $\alpha_\pi(t) = \epsilon$, implying decoupling of this trajectory at this particular value of t, as in the more familiar case of the ρ-trajectory at $t \approx -0.5$ where $\alpha_\rho(t) = 0$ and therefore $D_c(\alpha_\rho) = 0$. This pion decoupling occurs at small values of t satisfying $\alpha_\pi(t)-\epsilon = 0$, the small parameter ϵ being linearly proportional to the quantity $\delta = (\alpha_\rho(o)-\alpha_\pi(o))-0.5$. If the pion were exactly massless and the planar ρ-f trajectory intercept were exactly 0.5, so that $\delta = 0$, the pion decoupling would occur at $t = 0$ where $t_+ = t_-$: the coupling of a massless pion to two equally massive reggeons would vanish. Since at the planar level m_π^2 and δ are expected to be small, we expect this decoupling to occur at values of t close to $t = 0$. Chew and Rosenzweig[3,23] have conjectured that this type of mechanism may provide the analyticity-unitarity explanation of the origin of the Adler zero and with it of all the experimentally testable results of current algebra for purely hadronic processes, as shown by Mandelstam.[25]

By using the forms (23) and (24) for the reggeon coupling and propagator in Eq. (8) we have been able to obtain satisfactory self-consistency solutions. As in the case of the natural-parity ordered bootstrap, complete consistency for positive and negative values of t is obtained by introducing a smooth t-dependence e^{-at} associated with the triple Regge vertex.

As it was done in Eq. (15), let us define a function $\underline{P}(t)$ as the right-hand side of Eq. (8) times $D_c(\alpha_\pi)$, exact self-consistency

requiring $1 = P(t)$. In Figure 23 we show that it is possible to achieve self-consistency within 10% in the range $-.5 \leqslant \alpha^1 t \leqslant .6$ for the following values of the parameters: $\alpha_\rho(o) = 0.55$, $\alpha_\pi(o) = -0.02$, $\delta = 0.07$, $M^2 = 1 \text{ Gev}^2$, $a = -0.34$, $\varepsilon = -.09$.

4. The unnatural-parity cylinder

After obtaining self-consistent reggeon couplings and propagator we study the cylinder correction, following the same procedure as for the natural-parity cylinder. In this case, the cylinder shifts the $I = 0$ η and H trajectories, the $I = 1$ π-B trajectory remaining unchanged. Because the even charge-conjugation η is more massive than the π, unnatural-parity trajectories of even charge conjugation are shifted downwards from their planar values, exactly in the opposite direction of the cylinder displacement of the f-trajectory. This opposite sign of the unnatural-parity cylinder can be immediately understood from the unsymmetrical reggeon-loop model by considerations explained in section 6.

5. Model calculation of the π-η cylinder splitting

In the SU_2-symmetric model under consideration the cylinder-induced shifts of the $I = 0$ unnatural-parity trajectories η and H from the planar value $\alpha_0(t)$ are given by the non-linear equation

$$\alpha_{\eta,H}(t) = \alpha_0 \pm 2k(\alpha_{\eta,H}(t),t) \qquad (25)$$

where $\alpha_{\eta,H}(t)$ represents the output η and H-trajectories and the parameter $2k$ is to be associated with a twisted-reggeon loop according to Eq. (19). The values of the parameter $2k$ are shown in Figure 19 by the dashed curve and we can immediately compare it with the natural-parity cylinder represented by the continuous curve in the same figure. It is seen that at $t = 0$ the cylinder is of the same order of magnitude

in both natural and unnatural-parity sectors. However, in the positive-t region the unnatural-parity cylinder decreases at a much smaller rate. According to Chew and Rosenzweig this different behavior is responsible for the failure of the pseudoscalar mesons π, η, η^1 to exhibit planarity (exchange degeneracy, ideal nonet structure, isospin degeneracy) to the degree manifested by the leading natural-parity vector and tensor mesons.

The resulting η and H trajectories are shown in Figure 24. The cylinder-induced $\pi-\eta$ splitting is $m_\eta^2 - m_\pi^2 \approx .32$ which is of the same order of magnitude as the experimentally observed value.

6.   Sign of the unnatural-parity cylinder*

Jaime Millan[†]

Department of Physics and Lawrence Berkeley Laboratory, University of California, Berkeley, California 94720
(Received 22 December 1976)

We explain the sign difference between the natural-parity and the unnatural-parity cylinder by using a Reggeon-loop model proposed previously by Chew and Rosenzweig.

It is an empirical fact that the pseudoscalar mesons π, η, and η' display a deviation from "ideal" behavior strikingly different from the deviation exhibited by the vector and tensor mesons ρ, ω, ϕ, and A_2, f, f'. Not only is the magnitude of the deviation much larger for the pseudoscalars but the direction is opposite. For example, comparing particles of even charge conjugation, the $I=0$ f is *less* massive than the $I=1$ A_2 by ≈ 40 MeV, while the $I=1$ π is *more* massive than the $I=0$ η by ≈ 400 MeV. A comparison of mixing angles reveals a similar difference of magnitude and sign. In Refs. 1 and 2 the vector-tensor deviation from ideal, both in masses (or Regge intercepts) and in mixing angles, was discussed through the topological expansion and related to the so-called "cylinder." It has been pointed out[2,3] that the same general consideration should apply to unnatural-parity states, but no explanation has been given of the opposite sign that is experimentally required for the cylinder. The present note explains this sign difference through a Reggeon-loop model of the cylinder. The same model can be used to estimate the magnitude of the unnatural-parity cylinder, but we shall defer the question of magnitude to a subsequent lengthier paper. The sign is a simple matter, at least near $t=0$.

Positivity of total cross sections implies that the even-charge-conjugation natural-parity cylinder is positive at $t=0$.[2] In the context of a simple Reggeon-loop model with each link twisted as depicted in Fig. 1, this positivity emerges from the symmetrical character of the loop. Since both links of the loop correspond to the same

twisted (planar) Reggeon, the product of propagators at $t=0$, where $t_1 = t_2$, is positive. For the unnatural-parity cylinder, parity conservation at $t=0$ requires an unsymmetrical loop, one link carrying natural parity and the other link unnatural parity.[4] We now show that such an unsymmetrical loop, built from leading planar trajectories such as shown in Fig. 2, will have a sign opposite to that of a symmetrical loop.

We start from the general observation that, because planar discontinuities (of elastic amplitudes) are positive, the residues of the poles in a planar Reggeon propagator are all positive. For example, a familiar model for a planar propagator associated with a trajectory $\alpha_i(t_i)$, where the first physical particle occurs at $J=N_i$, is

$$S_i^P(t_i) = \exp\{-i\pi[\alpha_i(t_i) - N_i]\}\Gamma(N_i - \alpha_i(t_i)).$$

(1)

The alternation in sign of the Γ-function poles in formula (1) is compensated by the oscillating exponential factor. Twisted propagators, needed for the links of the Reggeon loops that build the cylinder through the model of Fig. 1 or 2, are obtained from corresponding planar propagators by adding a factor $\exp[+i\pi\alpha_i(t_i)]$:

$$S_i^{PX}(t_i) = \exp[i\pi\alpha_i(t_i)]S_i^P(t_i).$$

(2)

Such a factor makes negative the residues of all poles of odd J, leaving positive the even-J poles. For example, corresponding to the model planar propagator of formula (1), one has the model twisted propagator

$$S_i^{PX}(t_i) = (-1)^{N_i}\Gamma(N_i - \alpha_i(t_i)).$$

(3)

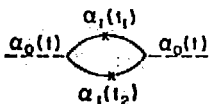FIG. 1. Symmetrical Reggeon-loop model of the natural-parity cylinder. The notation is the same as in Ref. 2.

FIG. 2. Unsymmetrical Reggeon-loop model of the unnatural-parity cylinder.

For the planar and the cylinder loop at $l = 0$ one requires l_1 and l_2 to be both negative. What sign may we expect for each twisted propagator? The sign is likely to be controlled at negative l_i by the residue of the nearest particle pole; i.e., that at $\alpha_i(l_i) = N_i$. The model of formula (3) exhibits this property. If this first particle has odd J, the twisted propagator is negative; when the leading particle has even J, the twisted propagator is positive. Therefore, for an unsymmetrical loop such as shown in Fig. 2, where the leading unnatural-parity particle (π) is even while the

leading natural-parity particle (ρ) is odd, the overall sign is negative.

The author wishes to thank Professor G. F. Chew for suggesting this work and for his continuous help, guidance and encouragement. He expresses his appreciation to the Rockefeller Foundation and Departamento de Fisica, Universidad del Valle, Cali, Colombia, for a Scholarship. He is also grateful to Professor J. D. Jackson for the warm hospitality at the Lawrence Berkeley Laboratory.

---

¹G. F. Chew and C. Rosenzweig, Phys. Rev. D 12, 3907 (1975).
²G. F. Chew and C. Rosenzweig, Nucl. Phys. B104, 290 (1976).
³T. Inami, K. Kawarabayashi, and S. Kitakado, Phys. Lett. 61B, 60 (1976).
⁴G. Goldstein and J. Owens, Nucl. Phys. B103, 145 (1976).

VIII.   SUMMARY AND CONCLUSION

In this work we have described self-consistent model calculations of ordered reggeon propagators and triple Regge couplings for natural-parity and unnatural-parity mesons by studying the multiperipheral ordered bootstrap of Rosenzweig and Veneziano. We have shown that after properly introducing the required threshold behavior of Regge vertices, it is possible to obtain solutions with different trajectory intercepts and slopes. We have calculated also cylinder shifts of planar trajectories and couplings, our results exhibiting the property that for the natural-parity mesons the cylinder diminishes rapidly as the energy increases, a phenomenon responsible for the remarkable regularities exhibited by the leading vector and tensor mesons such as exchange degeneracy, ideal mixing, slope and intercept of the pomeron.

We have attempted to extend the ordered bootstrap approach to the unnatural-parity mesons by using a simple model based on an unsymmetrical planar π-ρ helicity-pole loop. This model illustrates the fact that ordered unitarity, analyticity and Regge behavior relate the Adler condition for soft-pions to the intercept-difference of the π and ρ trajectories. We have studied the important properties of the unnatural-parity cylinder such as its sign, strength and behavior as a function of energy and showed that it explains qualitatively and quantitatively the puzzling properties of the pseudoscalar mesons.

Our results illustrate the possibility of fully determining the ordered S matrix and subsequent corrections from bootstrap constraints derived from ordered unitarity, analyticity and Regge behavior.

FIGURE CAPTIONS

Figure 1: Duality diagram representing a dual tree four-line connected part.

Figure 2: Example of a four-line connected part discontinuity.

Figure 3: Examples of quark-duality diagrams embedded in two-dimensional surfaces: (a) represents a cylinder and (b) a torus.

Figure 4: Example of an ordered S-matrix element S_0; p_i, m_i, t_i denote the momentum, mass and other quantum numbers (type) of particle i.

Figure 5: A four-line ordered connected part R.

Figure 6: Illustration of the property of factorization for the four-line ordered connected part of Figure 5. Each of the two factors in the residue of pole E is itself an ordered connected part.

Figure 7: Ordered cluster decomposition of an ordered S-matrix element.

Figure 8: Illustration of the property of ordered crossing for a four-line ordered connected part.

Figure 9: Definition of a four-line planar connected part $\underline{P}$ in terms of ordered connected parts.

Figure 10: Transition in ϕ-meson decay (a) allowed and (b) forbidden by the OZI rule, (c) the reaction illustrated in (b) becomes allowed at the cylinder level.

Figure 11: An n-particle intermediate-channel contribution to the S-discontinuity of a four-line ordered connected part R.

Figure 12: Diagram representing the multiperipheral region of phase-space for the ordered process $AB \to 1+2+...+n$. X_1 is the set of particles with rapidities $y_i > 0$ and X_2 is the set of particles having $y_i < 0$. Momentum transfer invariants t_i are limited to small values and particles 1 to n are approximately ordered in rapidity.

Figure 13: Schematic representation of the Regge expansion for each ordered connected part in the unitarity product of Figure 11.

Figure 14: Schematic representation of the derivation of the ordered bootstrap condition.

Figure 15: Graphical representation of the Rosenzweig-Veneziano ordered bootstrap equation.

Figure 16: The output trajectory (continuous line) obtained by Schaap and Veneziano in the numerical solution of the ordered bootstrap for an input trajectory $\alpha_{in} = .6 + \alpha^1 t$ (dashed line).

Figure 17: Graph of $P(t)$ vs. t for two different parametrizations of the function $g(t)$ appearing in Eq. (16). For $g(t) = $ constant we obtain the dashed line. For $g(t) = e^{-at}$ the continuous curve is obtained. Exact self-consistency requires $P(t) = 1$.

Figure 18: (a) Diagrammatic representation of a cylinder matrix

element connecting two planar Regge poles $|i>$

and $|j>$.

(b) Helicity-pole expansion of the matrix element

represented in (a), the twist denoting a

twisted link.

Figure 19: $Nk(t)$ vs. t for natural (continuous curve) and

unnatural- (dashed curve) parity cylinder.

Figure 20: The cylinder-shifted f, ω, ϕ and f^1 trajectories

(continuous lines). The dashed lines correspond

to the input planar trajectories $\alpha_0 = .5 + .95t$

and $\alpha_3 = .3 + .71t$.

Figure 21: $tg\theta\pm$ vs. t, $\theta\pm$ being the cylinder mixing angle

measuring the deviation of Regge couplings away

from their planar values.

Figure 22: Unsymmetrical reggeon-loop model for the ordered

bootstrap of the planar $\pi-\eta$ trajectory.

Figure 23: $P(t)$ vs. t for unnatural-parity bootstrap. Exact

self-consistency requires $P(t) = 1$ at each t.

Figure 24: The set of unnatural-parity trajectories H,π and

η at the cylinder level.

REFERENCES

1. G. Veneziano, Phys. Lett. 52B, 220 (1974); Nucl. Phys. B74, 365 (1974); Nucl. Phys. B117, 519 (1976).

2. Chan, H.M., J.E. Paton and Tsou S.T., Nucl. Phys. B86, 479 (1974). Chan, H.M., J.E. Paton, Tsou S.T. and Ng S. Wai, Nucl. Phys. B92 13 (1975).

3. G.H. Chew and C. Rosenzweig, Dual Topological Unitarization: an ordered approach to hadron theory, to be published in Physics Reports, and references therein.

4. G. Weissmann, private communication.

5. S. Okubo, Phys. Lett. 5, 165 (1963).

6. G. Zweig, CERN Report No. 8419/TH412, 1964 (unpublished).

7. I. Iizuka, K. Okado and O. Shito, Progr. Theor. Phys. 35, 1061 (1966).

8. S. Okubo, A review of quark-line rule, Univ. of Rochester report.

9. C. Rosenzweig and G. Veneziano, Phys. Lett 52B, 335 (1974).

10. J.R. Freeman and Y. Zarmi, Nucl. Phys. B112, 303 (1976). J.R. Freeman, Y, Zarmi and G. Veneziano, Nucl. Phys. B120, 477 (1977).

11. M. Bishari and G. Veneziano, Phys. Lett. 58B, 445 (1975).

12. G. Marchesini and G. Veneziano, Phys. Lett. 56B, 271 (1975). N. Ciafaloni, G. Marchesini and G. Veneziano, Nucl. Phys. B98, 472, 493 (1975).

13. M.M. Schaap and G. Veneziano, Nuovo Cim. Lett. 12, 204 (1975).

14. R.C. Brower, C.E. DeTar and J.H. Weis, Phys. Reports 14, 257 (1974).

15. G.F. Chew and C. Rosenzweig, Nucl. Phys. B104, 290 (1976).

16. P.D.B. Collins and E.J. Squires, Regge Poles in Particle Physics; Springer Tracts in Modern Physics, vol. 45.

17. M. Ciafaloni, C. De Tar and M. Misheloff, Phys. Rev. **188**, 2522 (1969).

    P. Lucht, the Generalized-Legendre addition theorems, $SU(1,1)$ and the diagonalization of convolution equations, LBL-5527 preprint, and private communication.

18. K. Konishi, Nucl. Phys. **B116**, 356 (1976).

19. G.F. Chew and C. Rosenzweig, Phys. Rev. **D12**, 3407 (1975), Nucl. Phys. **B104**, 290 (1976).

20. R. Hong Tuan, A consistency equation for the Pomeron, Laboratoire de Physique Théorique et Hautes Energies, Orsay, LPTHE 77/4 preprint.

    J.R. Freeman, Building a cylinder in the topological expansion, Univ. of Nebraska preprint.

21. Tsou S.T. Phys. Lett. **65B**, 81 (1976); Stony Brook preprint ITP-SB-77-31 (1977).

22. T. Inami, K. Kawarabayashi and S. Kitakado, Progr. Theor. Phys. **56**, 1570 (1976).

    C. Rosenzweig, Phys. Rev. **D13**, 3080 (1976).

    G.F. Chew and C. Rosenzweig, Phys. Lett. **63B**, 429 (1976).

23. G. Goldstein and J. Owens, Nucl. Phys. **B103**, 145 (1976).

24. G.F. Chew, unpublished and ref. 3.

25. S. Mandelstam, Phys. Rev. **168**, 1884 (1968).
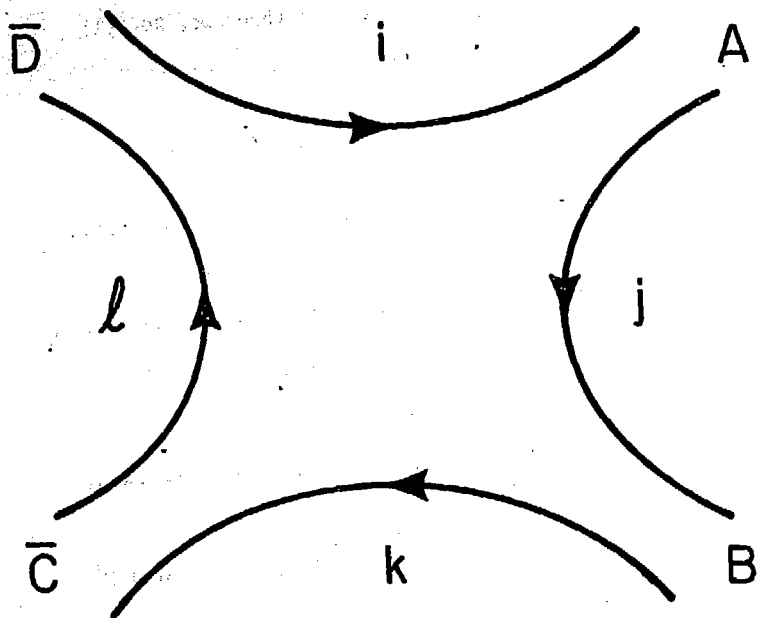
XBL7711-11020

Figure 1
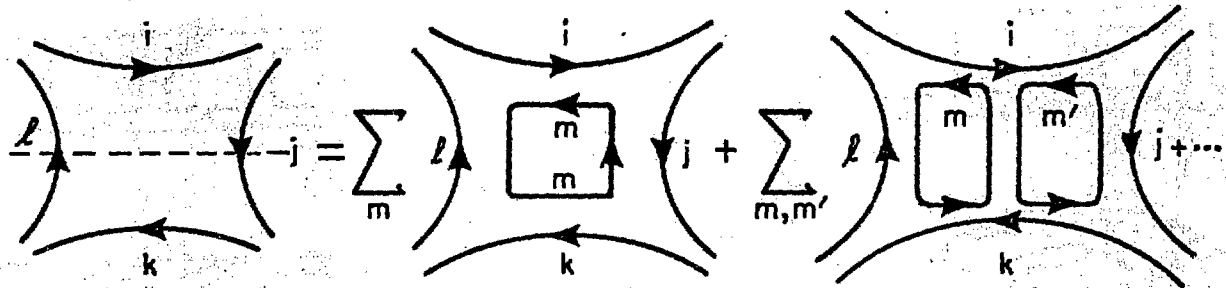
Figure 2

XBL7711-11030

Figure 3

(a)   (b)

42

t'_A, p'_A, m'_A ← S_O ← t_A, p_A, m_A

t'_B, p'_B, m'_B ← ← t_B, p_B, m_B
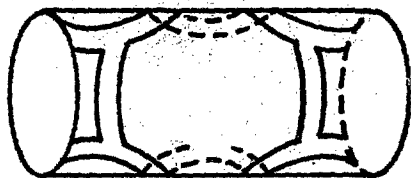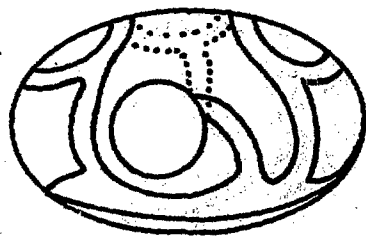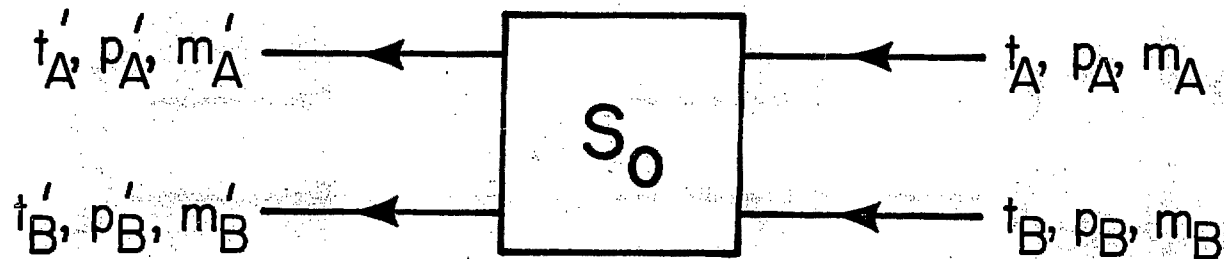
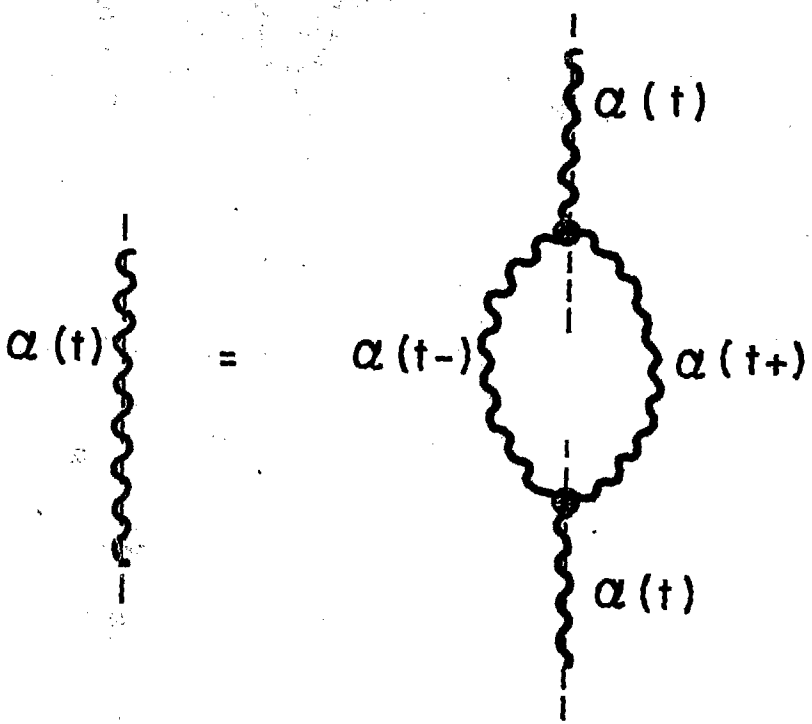Figure 4

XBL 7711-11021

43
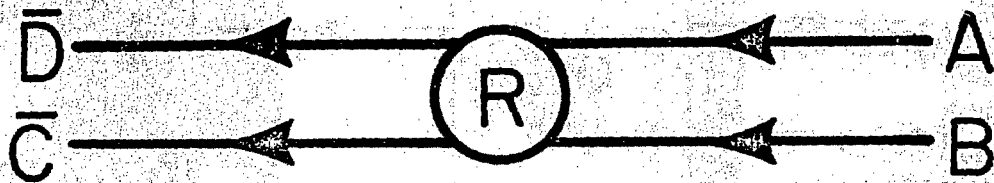
Figure 5

XBL 7711-11019
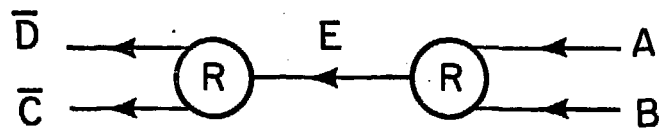
XBL 7711 - 11031

Figure 6
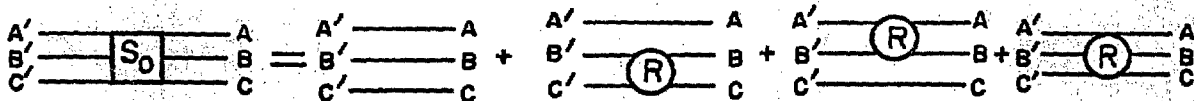
Figure 7

XBL7711-11025

46
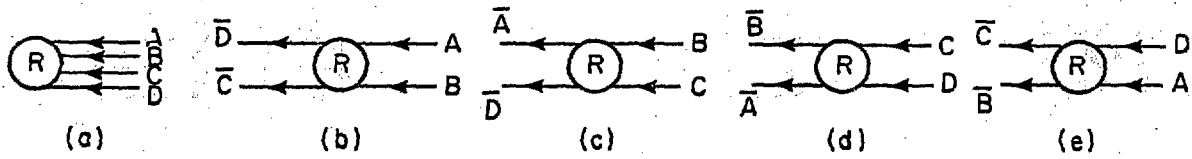
Figure 8
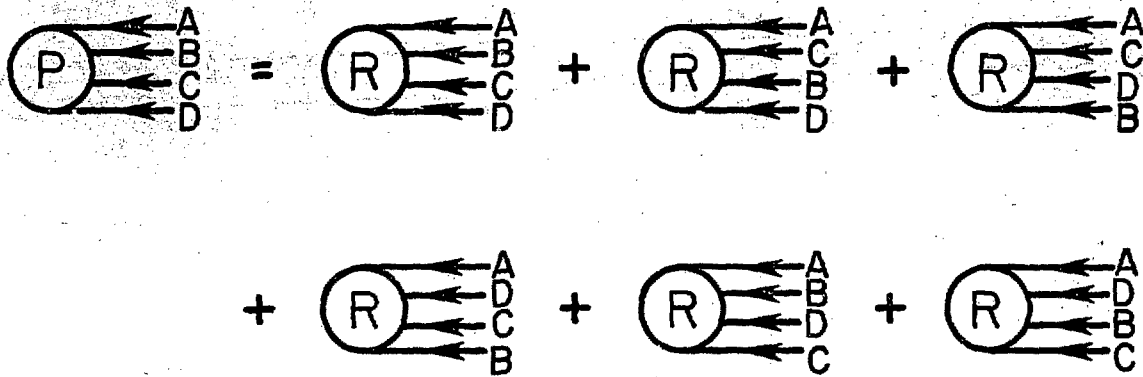
XBL7711-11018

Figure 9

(a)   (b)   (c)
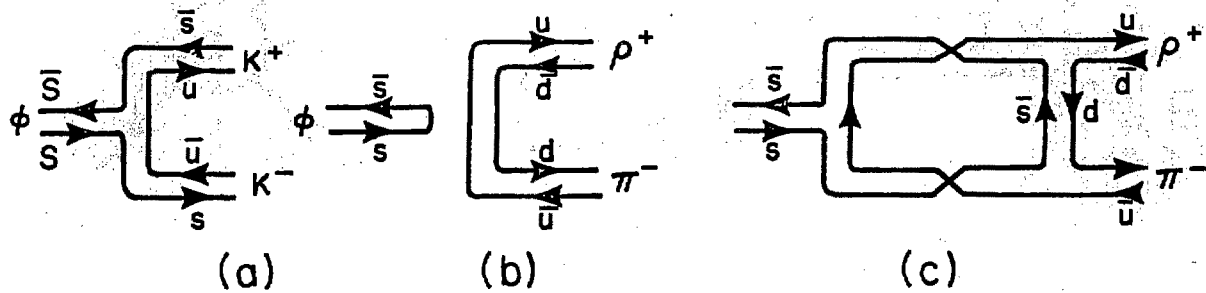
Figure 10

Figure 11

XBL77II-11017

50
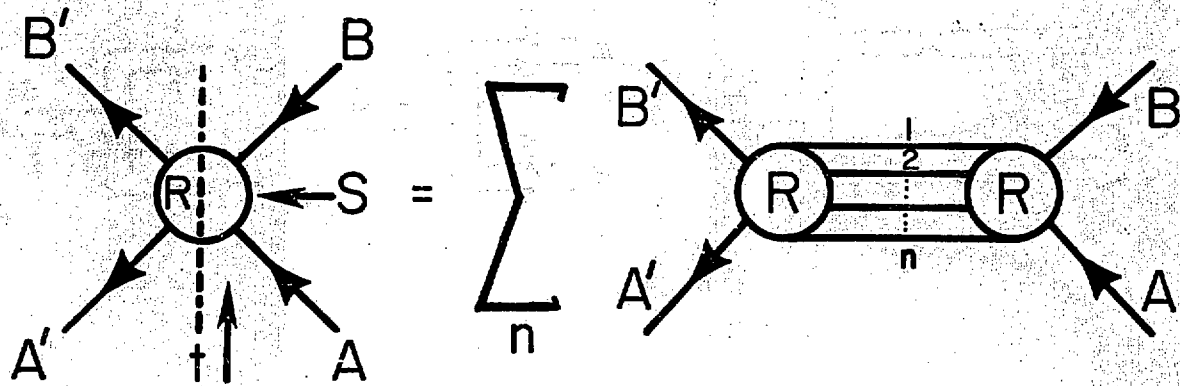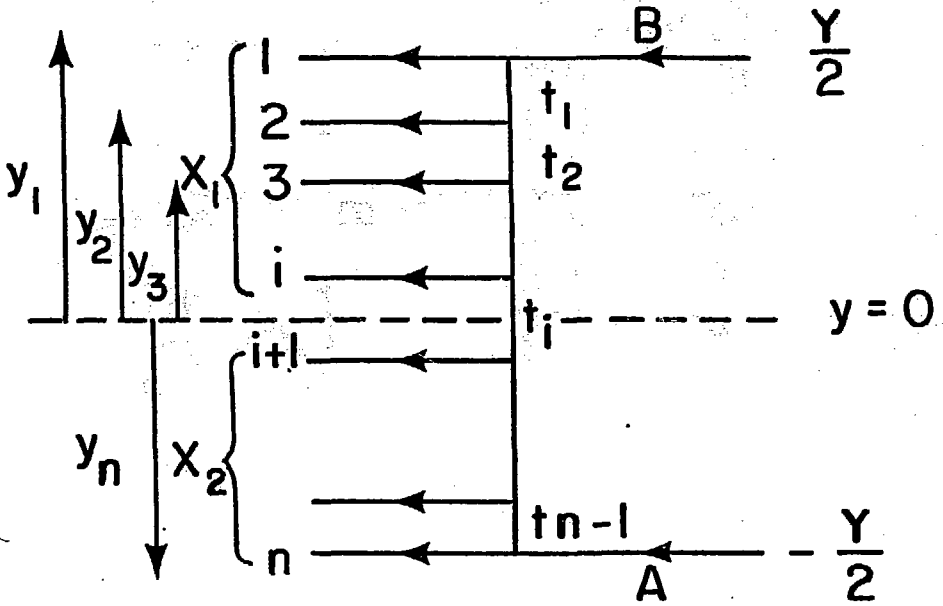
XBL7711-11026

Figure 12

Figure 13

52
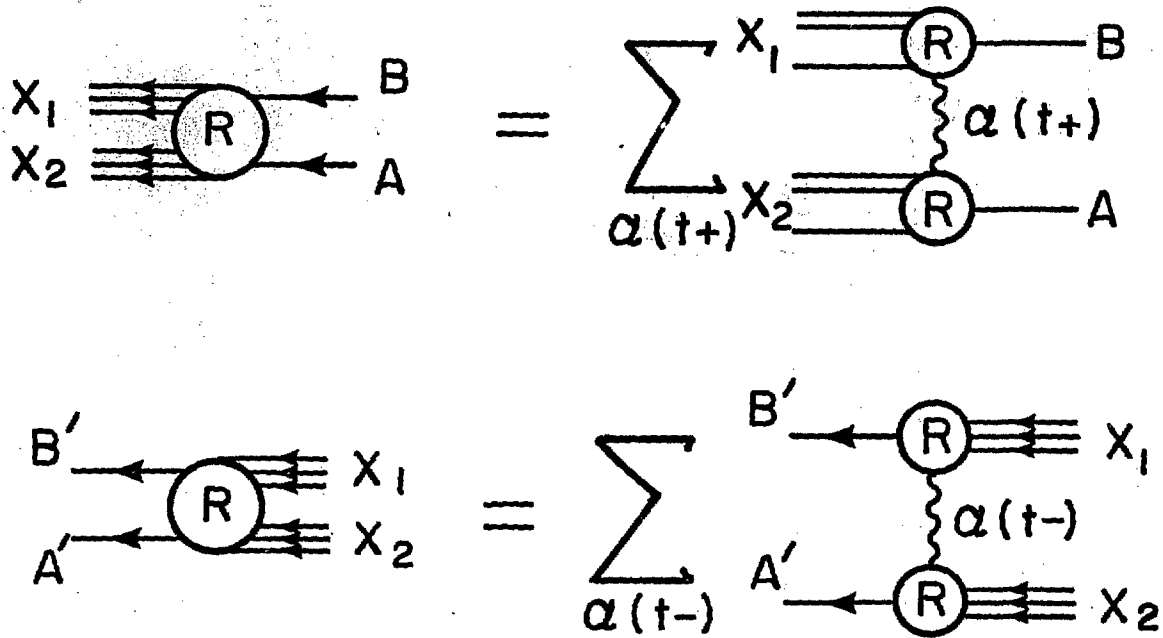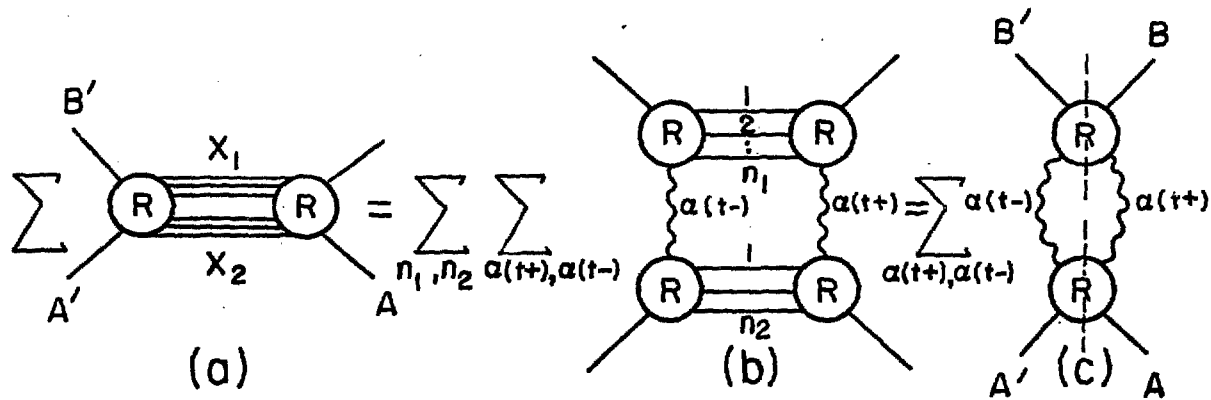
Figure 14

XBL 7711-11029

53

Figure 15

XBL 7711-11012
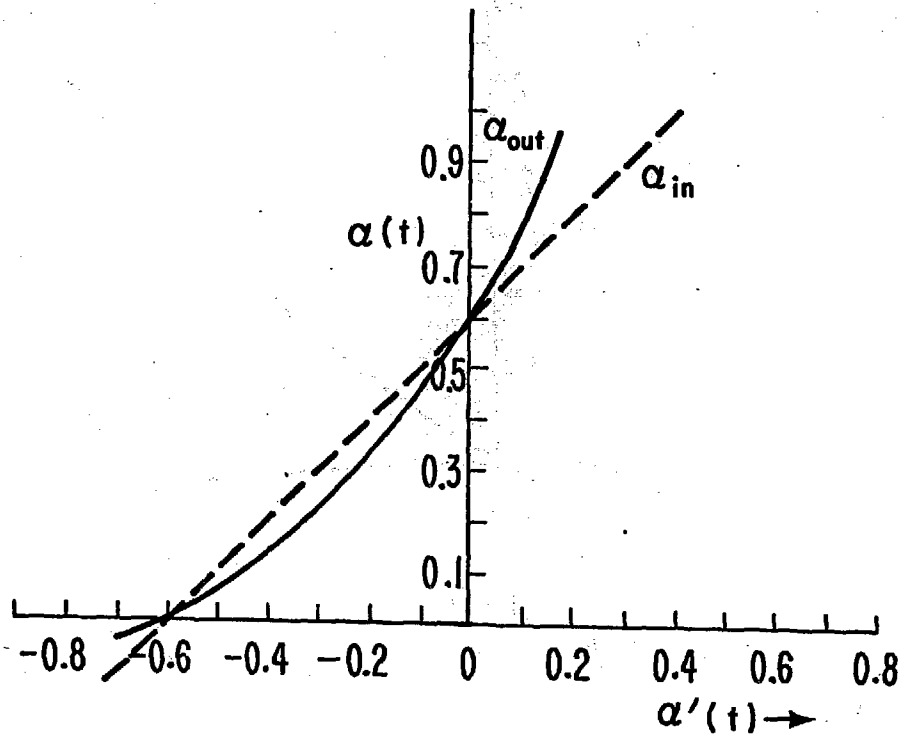
Figure 16

XBL 7711-11014
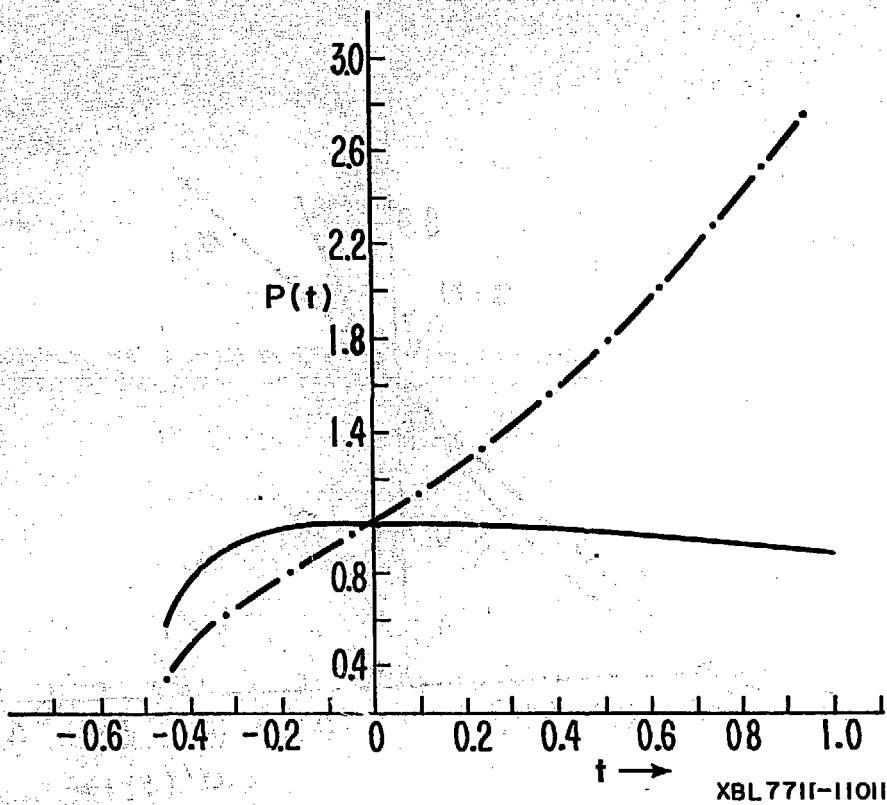
Figure 17
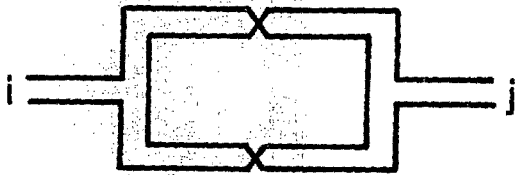
XBL 7711-11011

(a)
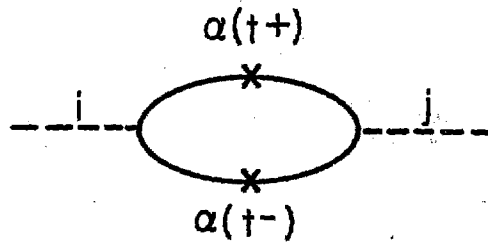
(b)

$\alpha(\dagger+)$

$\alpha(\dagger-)$

Figure 18

XBL7711-11016
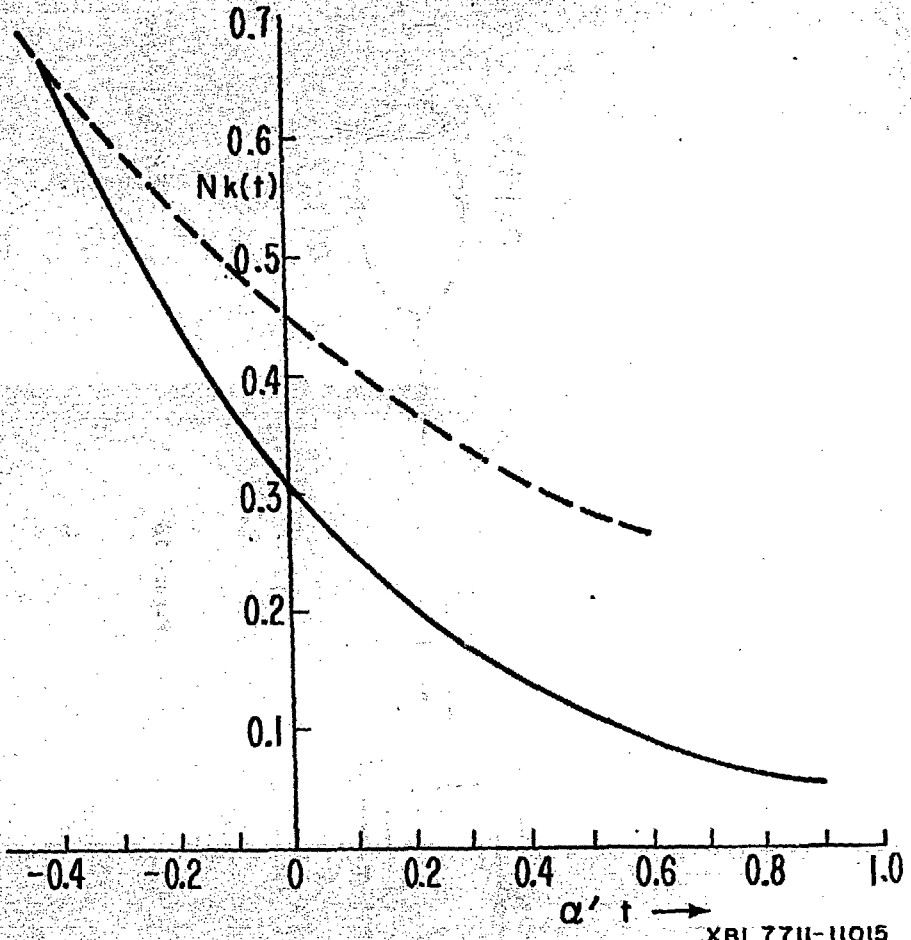
Figure 19

XBL 7711-11015
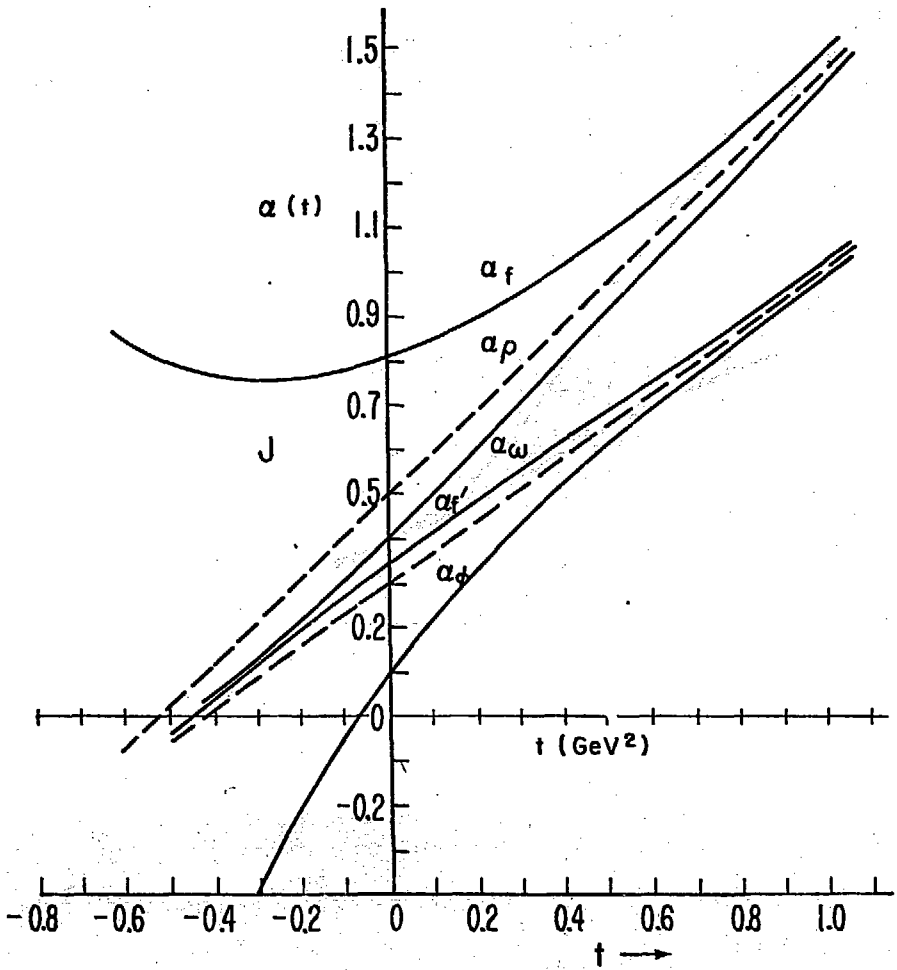
Figure 20

XBL7.711-11009
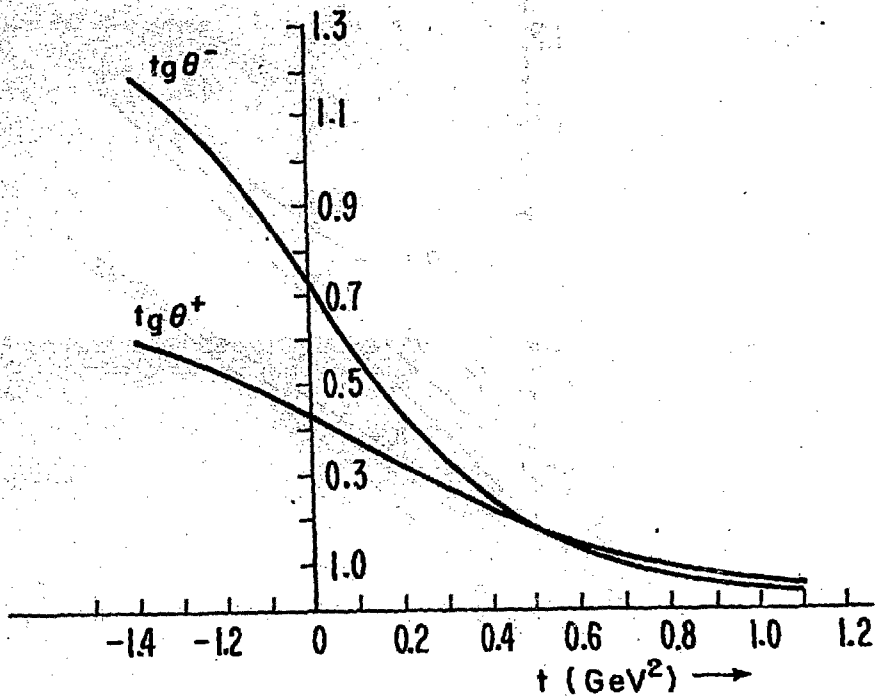
XBL7711-11024

Figure 21

$\alpha_\pi(t+)$

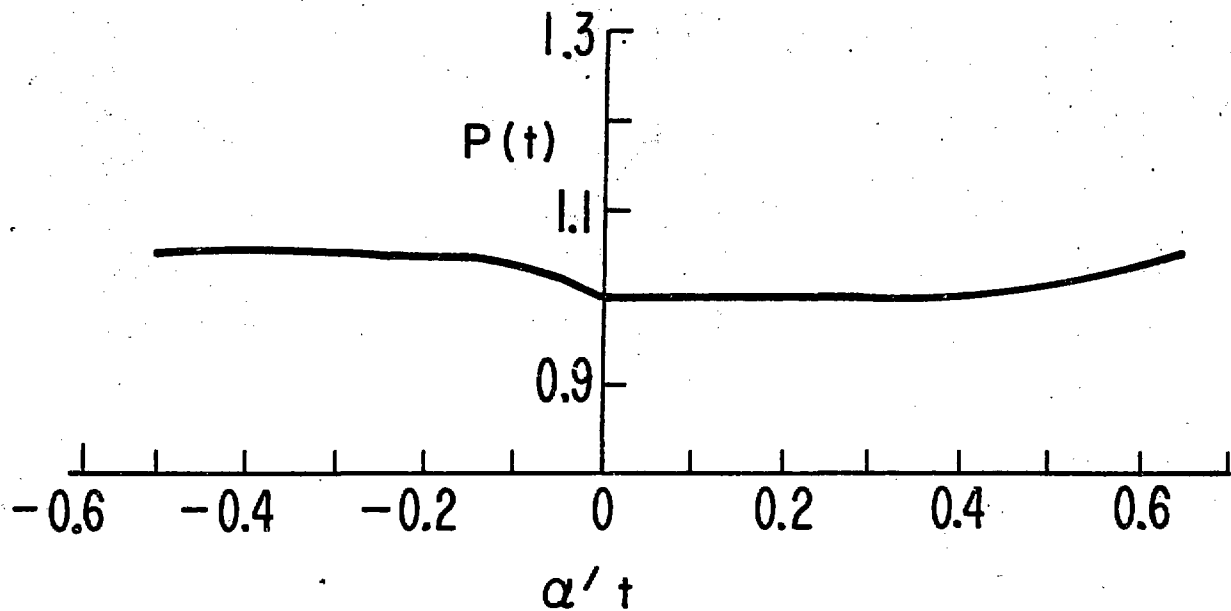$\alpha_\pi(t)$
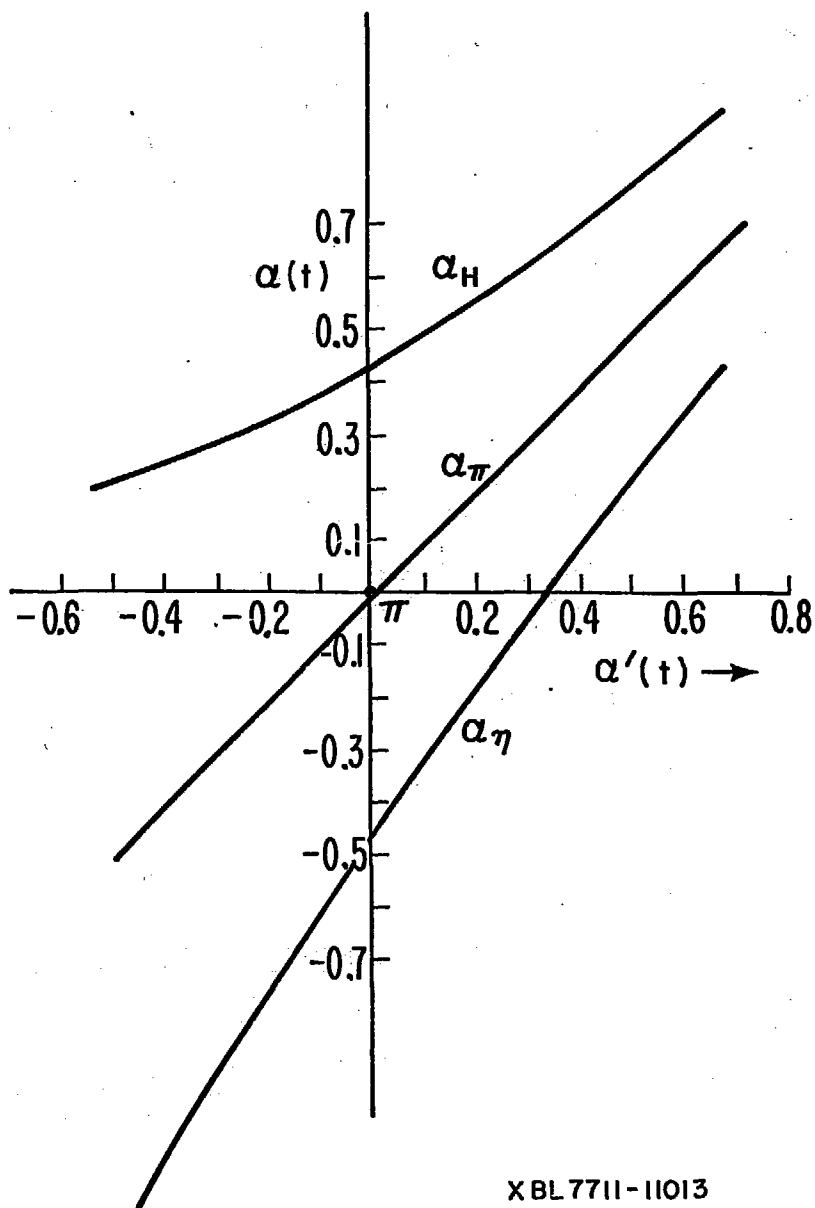
$\alpha_\pi(t)$

$\alpha_\rho(t-)$
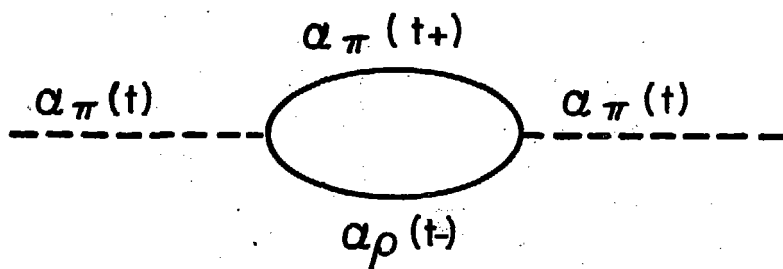
XBL7711-11008

Figure 22

Figure 23

XBL 7711-11023

XBL 7711-11013

Figure 24